Characterization of Polymer Composites between Stereocomplex Polylactide Blends with Poly (methyl methacrylate)

Onpreeya VEANG-IN [1], Yottha SRITHEP [1]*, **John MORRIS [2], Dutchanee PHOLHARN [3]**

[1] *Manufacturing and Materials Research Unit, Department of Manufacturing Engineering, Faculty of Engineering, Mahasarakham University, Mahasarakham 44150, Thailand*
[2] *School of Industrial Education and Technology, King Mongkut's Institute of Technology Ladkrabang, Bangkok, 10520, Thailand*
[3] *Department of Chemistry, Faculty of Science and Technology, Rajabhat Maha Sarakham University, Mahasarakham 44000, Thailand*

Polylactide stereocomplex (ST) of poly(L-lactide) (PLLA) and poly(D-lactide) (PDLA) (PLLA:PDLA 50:50) was blended with poly(methyl methacrylate) (PMMA) $10-50$ wt.%. The materials were dissolved in chloroform at room temperature and the films were then cast. Differential scanning calorimetry showed a stereocomplex melting peak at 208 °C – 50 °C higher than that for neat PLLA or PDLA - confirming the polylactide stereocomplex crystallites. The PMMA content ratio of $10-50$ wt.% in the stereocomplex showed almost complete stereocomplex crystallites. A peak at about 908 cm^{-1} in Fourier transform infrared spectra further confirmed the stereocomplex crystallites which indicated that PMMA could blend and efficiently bond with the stereocomplex. The X-ray diffraction analysis showed that the stereocomplex crystallinity became smaller when PMMA was added. Morphology from scanning electron microscopy revealed that phases separated in the ST/PMMA blend when the amount of PMMA was increased. Adding PMMA to stereocomplex films led to an increased elongation at break which peaked at 30 % added PMMA. Increased PMMA also led to the improved thermal stability of the stereocomplex. These properties and higher toughness are also needed in common applications, in particular films for packaging and protection of manufactured products.
Keywords: stereocomplex polylactide, poly (methyl methacrylate), thermal and tensile properties.

1. INTRODUCTION

Biodegradable polymers are important alternatives to conventional petrochemical-based polymers. Polylactides are considered interesting and promising biodegradable materials [1]. Poly(L-lactide) (PLLA) is a thermoplastic polyester, made from fermented plant starch, e.g. corn, cassava, sugarcane or sugar beet pulp, which is easy to process and has good mechanical properties, yet degrades naturally in the environment [2]. Thus, the control of the mechanical properties and thermal behaviour based on studying structure and morphology is a key topic. The applications of pure PLLA are restricted by its thermal properties, low toughness and poor elongation at break [2, 3]. To overcome these limitations, blending PLLA with other polymers is an inexpensive approach that tailors the final properties of the composition. Moreover, miscible blends of PLLA and PDLA, which lead to stereocomplex crystals, are the basis of this study.

In recent years, poly(methyl methacrylate) (PMMA) has been extensively used in the fabrication of artificial dentures, tissue engineering and ophthalmic intraocular lenses. Zhang et al. [1] explored the miscibility of PLLA and PMMA through solution precipitation and solution casting methods. From precipitation, they achieved full miscibility, whereas casting led to two separate phases. Imre et al. [3] compared PLLA with $10-90$ % polystyrene (PS) and PLLA with $10-90$ % PMMA blends: the dispersed particle sizes differed significantly, indicating dissimilar interactions for the corresponding pairs. The PLLA/PMMA blends with the smallest dispersed particles exhibited the highest tensile strength, whereas PLLA/PS blends with the coarsest structures had the lowest strength. The interfacial interaction was the strongest for the PLLA/PMMA pair and weakest for PLLA/PS.

Many researchers studied the application of PLLA by improving thermal and mechanical properties, such as the formation of stereocomplex [4 – 6]. A promising technique to enhance the properties of PLLA is blending a 1:1 ratio of PLLA to PDLA with reinforcing elements by the interaction between polymers for inducing the stereocomplex crystal structures [5]. The stereocomplex crystals exhibit improved thermal properties compared to pure PLLA or PDLA homocrystallites. The stereocomplex had a higher melting temperature and a higher crystallization temperature, by more than 50°C and 25°C, respectively [6]. It was reported that the PLLA and PDLA (50/50 wt%) with $30-40$ %PMMA could be mixed by fusing the mixtures in twin-screw extruders on the first inspection [7]. However, in this work, we formed films and showed that the formation of stereocomplex crystals improved thermomechanical properties that were effectively developed from high-molecular-weight PLLA, PDLA, and PMMA blends.

---

* Corresponding author. Tel.: +66-91-0614566; fax: +66-43-754316
E-mail address: yottha.s@msu.ac.th (Y. Srithep)

In this study, we prepared equal quantities of PLLA and PDLA blend to form a streocomplex, with effect of PMMA 10 – 50 wt.% addition to stereocomplexation by solution casting. In addition, the chemical structure, mechanical and thermal properties of the mentioned blends films were investigated.

2. EXPERIMENTAL

2.1. Materials

PLLA (trade name L175) and PDLA (trade name D120) were received from Total Corbion Thailand Ltd. PMMA (grade CM205) was received from Chi Mei Corporation, Taiwan. Chloroform (CHCl₃) was supplied by RCI Lab scan Limited, Thailand.

2.2. Processing

To prepare the samples, PLLA, PDLA and PMMA were dried in a vacuum oven at 80 °C for 24 h. The PLLA/PDLA/PMMA blends (100/0/0, 50/50/0, 45/45/10, 35/35/30, 25/25/50, and 0/0/100) were dissolved at a concentration of 1 g of the materials in 10 mL chloroform (magnetically stirred, 3 hours, 25 °C). The solutions were cast onto Petri dishes. The films were dried (24 h, 25 °C) to allow the solvent to evaporate. Final film thicknesses were measured approx 0.3 mm. The resulting films were cloudy, strong (see measured tensile strengths later), and elastic.

2.3. Characterization

2.3.1. Fourier transform infrared spectroscopy (FTIR)

Details of the components of the chemical structures of the blends were obtained with a Perkin Elmer Frontier FTIR spectrometer, scanned from 400 to 4000 cm^{-1}, in the attenuated total reflection mode.

2.3.2. X-ray diffraction analysis (XRD)

Sample crystallinities were determined from X-ray diffraction with an Analytical Bruker/D8 Advance Bruker-BioSpin (Cu Kα line source, filtered with a thin Ni filter, scanned at 2°/min, 2θ from 5 – 40°). Film samples were mounted on the XRD platform and the computer-controlled goniometer was run in wide-angle mode.

2.3.3. Differential scanning calorimetry (DSC)

Film thermal properties were measured by DSC (Pyris Diamond DSC4000, MA, USA). Samples weighing 3 to 5 mg. were placed in aluminum pans and sealed. The samples were heated from 25 °C to 250 °C at a rate of 10 °C/min, held for 3 min at 250 °C (first heating cycle) and cooled at 10 °C/min to 25 °C. The samples were reheated to 250 °C at 10 °C/min (second heating cycle). The cold crystallization temperature (T_{cc}) and its enthalpy, homo-melting temperature (T_{m1}) and its enthalpy (ΔH_{m1}), stereocomplex melting temperature (T_{m2}) and its enthalpy (ΔH_{m2}), the crystallization temperature (T_c) and its enthalpy were recorded. The glass transition temperature (T_g) was determined from the second scan. The total degree of crystallinity (X_c) for both the homo- and stereocomplex-crystals was calculated with Eq. 1 [8]:

$$Xc\ (\%) = \frac{\Delta Hm,hc + \Delta Hm,st - \Delta Hcc}{w \times \Delta H^0_{m(blend)}} \times 100\%, \qquad (1)$$

where $\Delta H_{m,hc}$ and $\Delta H_{m,st}$ are the melting enthalpies of homocrystallites and the stereocomplex crystallites, respectively; ΔH_{cc} is the cold crystallization enthalpy; w is the weight fraction of PLLA or the stereocomplex in the polymer blends; $H^0_{m(blend)}$ is the theoretical value of the melting enthalpy for perfect crystals, which can be calculated as follows:

$$H^0_{m(blend)} = H^0_{m,hc} \times f\text{hc} + H^0_{m,st} \times f_{st}, \qquad (2)$$

where $H^0_{m,hc}$ and $H^0_{m,st}$ are the enthalpy value for the homocrystallites (93.6 J/g) and the stereocomplex crystallites (142 J/g), respectively; f_{hc} and f_{st} are the relative amounts of the homo- and streocomplex crystallites, respectively, using under nonisothermal conditions, and can be calculated according to Eq. 3 and Eq. 4:

$$f_{hc}\ (\%) = \frac{\Delta Hm,hc}{\Delta Hm,hc + \Delta Hm,st} \times 100\%; \qquad (3)$$

$$f_{st}\ (\%) = \frac{\Delta Hm,st}{\Delta Hm,hc + \Delta Hm,st} \times 100\%, \qquad (4)$$

where the $\Delta H_{m,hc}$ and $\Delta H_{m,st}$ values were obtained from the thermograms as for Eq. 1. The crystallinity of stereocomplex crystallites (X_{st}) was then calculated (Eq. 5) from the f_{st} calculated in Eq. 4:

$$X_{st}\ (\%) = X_c \times f_{st} \times 100\%. \qquad (5)$$

2.3.4. Scanning electron microscopy (SEM)

0.3 mm thick films were cryogenically fractured cross-section surface to expose the internal structure, sputtered with a ~ 20 nm layer of gold and SEM images were captured by SEM (TM4000Plus Tabletop Microscope, HITACHI) under 1000× magnification.

2.3.5. Mechanical testing

15 mm × 50 mm samples were cut from the films. The modulus of elasticity, tensile strength, and elongation at break were measured at 25 ± 2 °C on a tensile tester (Texture Analyzer, TA.XT Plus) at a crosshead speed of 2 mm/min. Means and standard deviations for five replicates of each sample were reported.

2.3.6. Thermogravimetric Analysis (TGA)

Thermal properties were measured by TGA (PerkinElmer, TGA4000, MA, USA) from 30 to 600 °C at 10 °C/min under a constant N₂ flow. Each test used 10 – 15 mg of the films. Mass loss was recorded and normalized against the initial mass. The temperature at 5 % weight loss ($T_{5\%}$) was reported as the decomposition temperature.

3. RESULTS AND DISCUSSION

3.1. Chemical structure

Fig. 1 a shows the FTIR spectra of the blends. PMMA spectra identified the functional groups present in the

synthesized PMMA. A sharp intense peak at 1.731 cm^{-1} showed the presence of the acrylate carboxyl group. The broad peak from 1.260 – 1.000 cm^{-1} was attributed to the |C-O (ester bond) stretching vibration.

a

b

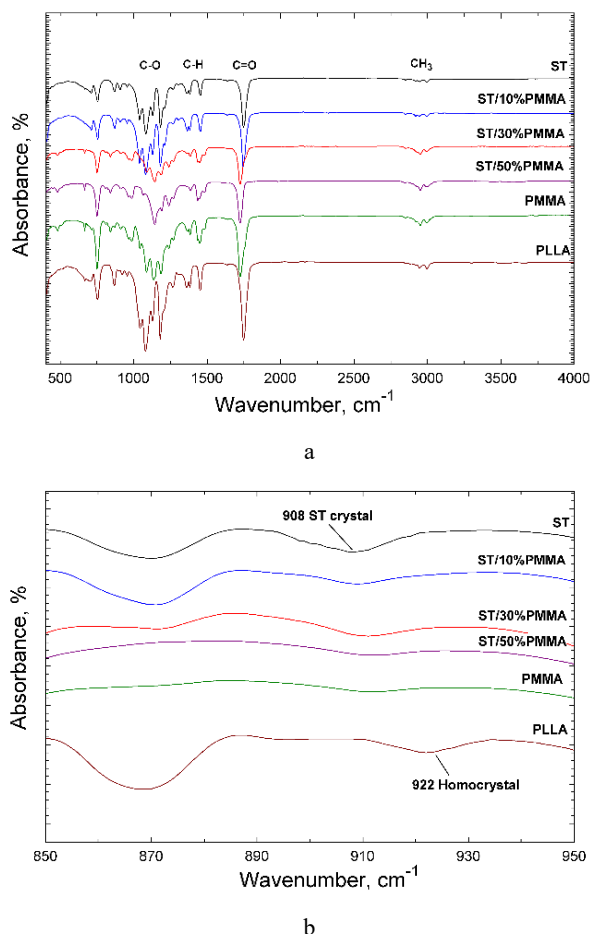**Fig. 1.** FTIR spectra: a – PLLA, ST, PMMA, and ST/PMMA blends; b – expanded region from 850 to 950 cm^{-1}

The band at 1.433 cm^{-1} was attributed to C-H stretching vibrations of the CH$_3$ group. The 2.950 cm^{-1} band can be assigned to the bending vibrations of the CH$_3$ groups [9]. The ST sample had a strong peak corresponding to carbonyl (C=O) stretching at 1.744 cm^{-1} [10]. After ST and PMMA were blended, the FTIR spectrum contained absorption peaks at similar locations to those of pristine ST and PMMA. The C-O stretching vibrations of the blends, that were not compatible, showed a split peak with similar intensities at 926 and 986 cm^{-1}. The presence of this split peak indicates the presence of both polymers in the blend. When loading of PMMA increased, the infrared spectrum of ST/50%PMMA appeared very close to PMMA, which may indicate some intramolecular interactions between the PMMA and ST. In addition, ST and PLLA show a peak with similar, but wave range extends number from 850 to 950 cm^{-1} were different as shown in Fig. 1 b. Fig. 1 b (expands the region from 850 to 950 cm^{-1} of Fig. 1 a) shows the neat PLLA with an obvious peak of about 922 cm^{-1}, assigned to the PLLA homocrystallites [11]. When PLLA and PDLA were blended, stereocomplexes formed, confirmed by a peak appearing at about 908 cm^{-1} assigned to the stereocompex crystallites [12]. This peak became weaker as the PMMA content increased.

3.2. X-ray diffraction analysis

XRD diffractograms are shown in Fig. 2. PLLA had 2θ reflections at 16.7° and 19.2° [13].
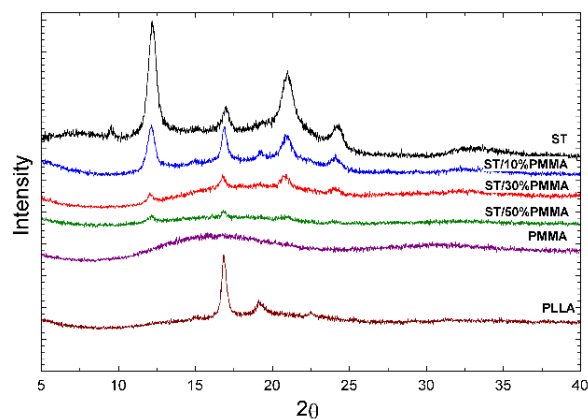

Fig. 2. XRD profiles of PLLA, ST, PMMA, and ST/PMMA blends

Peaks at 11.68°, 20.68° and 23.58° were assigned to planes of the stereocomplex crystallites [14]. PMMA showed large scattering, the center of the peak at about 14.3° and 31.7° indicated that PMMA structure was amorphous [15]. When the stereocomplexes were mixed with PMMA, all the diffraction peaks of the blends gradually became smaller or essentially disappeared as the amount of PMMA increased. This indicated that the film became amorphous and the degree of crystallinity of the polymer decreased.

3.3. Thermal properties

3.3.1. First heating cycle

Fig. 3 shows the DSC thermograms of the films and Table 1 summarizes the data. The neat PLLA had a melting peak (T_{m1}) at ~ 175 °C. The pure PMMA revealed a typical amorphous behavior with no melting temperature and had a glass transition temperature at ~ 98 °C [16].
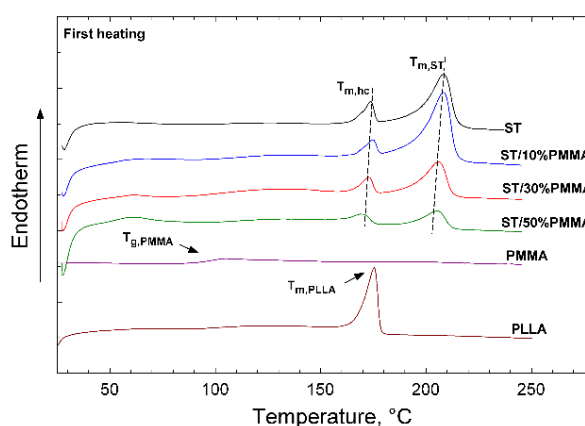

Fig. 3. DSC first heating thermograms of ST, PMMA, and ST/PMMA blends

In the stereocomplex, two T_m peaks were observed: the first peak was the homocrystallites, T_{m1}, melted at ~ 173 °C and the second was the stereocomplex crystallites, T_{m2}, melted at ~ 208 °C. The stereocomplex structure moved the melting temperature higher that than of PLLA by ~ 50 °C [6, 17]. This significant increase is due to hydrogen bonding interactions in the stereocomplex crystalline structure [6].

Table 1. DSC first heating data of PLLA, ST, PMMA, and ST/PMMA blends film

| Sample | T_g, °C | Melting 1 | | Melting 2 | | $\%X_c$ | $\%X_{st}$ |
		T_{m1}, °C	$\Delta H_{m.hc}$, J/g	T_{m2}, °C	$\Delta H_{m.st}$, J/g		
ST	–	173.6	5.4	208.2	38.1	32.0	28.0
ST/10%PMMA	–	174.6	3.8	208.2	29.4	27.0	23.8
ST/30%PMMA	–	172.8	4.3	205.9	19.5	25.5	20.8
ST/50%PMMA	–	170.4	3.4	205.4	8.8	19.0	13.6
PMMA	98.5	–	–	–	–	–	–
PLLA	–	175.60	31.1	–	–	33.2	–

When PMMA was added 10 to 50 wt.% to the stereocomplex, the samples also showed two T_m points, and the enthalpy of melting of both ΔH_{m1} and ΔH_{m2} decreased as the amount of PMMA increased. The crystallinity (X_c) of PLLA was 33.2 % due to the slow cooling in casting the film. Furthermore, the total degree of crystallinity (X_c) of ST was 32.0 % and the crystallinity of the stereocomplex crystallites (X_{st}) of ST was 28.0 %. The crystallinity of the blends reduced gradually as the PMMA content increased and pure PMMA became fully amorphous.

3.3.2. Cooling cycle

Fig. 4 shows the crystallization temperatures, T_c, on cooling. PLLA, PMMA and ST/PMMA blends were difficult to crystallize, no clear crystallization was observed upon cooling.
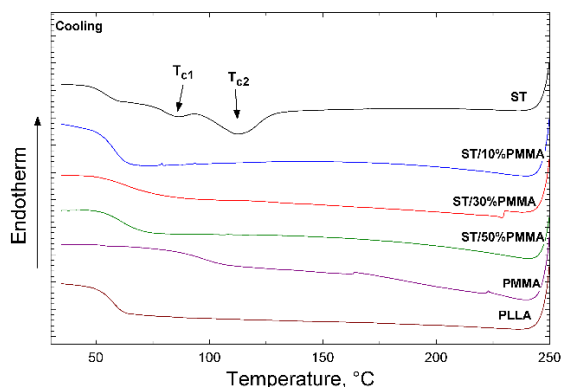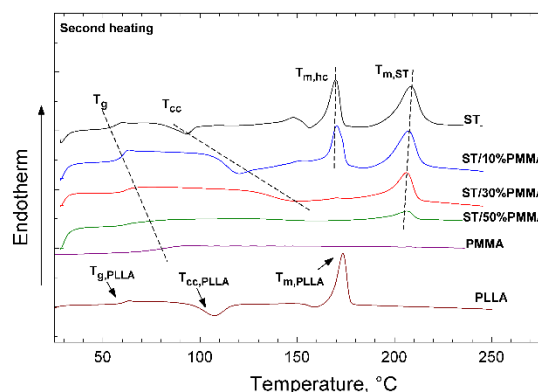

Fig. 4. DSC cooling thermograms of ST, PMMA, and ST/PMMA blends

However, the stereocomplex had two crystallization peaks, with T_c's at 112.6 and 85.6 °C. This might be the crystallization of homocrystal and stereocomplex crystals indicating that both homocrystallites and stereocomplex

crystallites formed and the crystallization enthalpies, ΔH_c, were 6.2 and 0.8 J/g, respectively. This indicated that the PLLA and PDLA of ST were easily separable [18].

3.3.3. Second heating cycle

Fig. 5 and Table 2 show the thermograms of the second heating cycle for the PLLA, ST, PMMA and ST/PMMA blend films.

Fig. 5. DSC second heating thermograms of ST, PMMA, and ST/PMMA blends

The deterioration of the material during heating led to lower melting points and enthalpies of all samples than those from the first heating cycle [19]. During the second heating, the glass transition temperature point was clearly observed, due to faster cooling than the first heating scan and increased with the addition of more PMMA. The stereocomplex had a glass transition, T_g, at 57.1 °C. When it was mixed with 50%PMMA, the T_g increased to 65.2 °C. With increased amounts of PMMA, the ability of the stereocomplex to cold crystallize also systematically decreased and the point of cold crystallization shifted to a higher temperature [20].

Table 2. DSC second heating data of PLLA, ST, PMMA, and ST/PMMA blends film

| Sample | T_g, °C | Cold crystallization | | Melting 1 | | Melting 2 | | $\%X_c$ | $\%X_{st}$ |
		T_{cc}, °C	ΔH_{cc}, J/g	T_{m1}, °C	ΔH_m, J/g	T_{m2}, °C	ΔH_m, J/g		
ST	57.1	92.8	5.6	169.5	15.4	208.3	25.9	28.8	18.1
ST/10%PMMA	60.8	119.8	20.0	170.4	14.8	207.1	23.8	16.7	10.2
ST/30%PMMA	61.3	148.0	7.9	-	–	206.1	17.3	–	9.6
ST/50%PMMA	65.2	–	–	–	–	206.5	5.5	–	7.7
PMMA	99.6	–	–	–	–	–	–	–	–
PLLA	61.1	107.2	13.3	173.4	25.5	–	–	13.0	–

ST/50%PMMA samples showed no cold crystallization, homocrystals disappeared and fewer stereocomplex crystals formed. The T_m of the films changed slightly to a lower temperature with increasing amounts of PMMA. Moreover, ST/30%PMMA, ST/50%PMMA showed a complete stereocomplex structure without any homocrystallites and $T_m \sim 206$ °C. The smaller crystallite enthalpy implied a reduction of crystallization.

3.4. Morphology

The morphology of PLLA, ST and ST/PMMA blends was examined by scanning electron microscopy (see Fig. 6). The PLLA, ST and PMMA samples (Fig. 6 a, b, and f) showed a smooth fracture surface, the morphology is highly homogeneous, a relatively brittle morphology after a fracture. When the ST blended with PMMA 10 and 30 wt.% as shown in Fig. 6 c and d, the surfaces showed craggy and exhibited more ductile behavior than the pure polymer. On the other hand, when the content of the PMMA increased to 50 wt.%, the surface morphology changes, larger PMMA particles appeared on the fracture surface, indicating that PMMA promoted phase separation [9], and poor compatibility.

3.5. Tensile test

Fig. 7 shows the results of tensile tests on solution cast films made of PLLA, ST, PMMA and ST/PMMA blends. PMMA was introduced to enhance the mechanical properties of polylactide stereocomplex, hypothesizing that PMMA would serve as a reinforcement to enhance the physical cross-linking points and confine the polymer chain motion and facilitate good interaction between the stereocomplex matrix and the PMMA [21].

As shown in Fig. 7 a, neat PLLA had a tensile strength of ~ 19 MPa, whereas the stereocomplex was much stronger at ~37 MPa. Tsuji et al. and Xu et.al. [22, 23] measured the mechanical properties of pure PLLA/PDLA blends and showed that the mechanical strength of stereocomplexes was almost 60 % higher than that of PLLA. Furthermore, pure PMMA had a tensile strength of ~ 36 MPa, adding PMMA 10 – 50 wt.% into the stereocomplex increased the tensile strength to similar a similar level at 34 – 35 MPa.

Fig. 7 b shows the change of Young's modulus as more PMMA was blended into the stereocomplex. An increase in PMMA content resulted in a gradual increase of Young's modulus. The lowest moduli were ~ 3.6 MPa for neat PLLA, while the stereocomplex showed ~ 4.2 MPa, and the highest was ~ 6.8 MPa for PMMA. When the amount of PMMA increased, the tensile modulus of films increased. Similar results were reported in a study of the increase in PMMA content in PLLA/PMMA blends and PMMA monotonically increased the tensile modulus and tensile strength of the resulting material [24].

Fig. 7 c shows that the elongation at break of neat PLLA was 192 %, ST was 187 %, and PMMA was 51 %. For the stereocomplex blended with 30 wt.% PMMA, it increased by 383 %. López-Rodríguez et al. [25] also reported that a blend of pure PLLA and PMMA enhanced the strength and elongation at thebreak due to a high density of intercrystalline connections through a mobile amorphous phase. On the other hand, when adding PMMA at 50 wt.% content to PLLA, the elongation at break started to decrease. This suggested that the PMMA was dispersed well at concentration levels below 50 wt.%, but, when further PMMA was added, the blended films became brittle again.
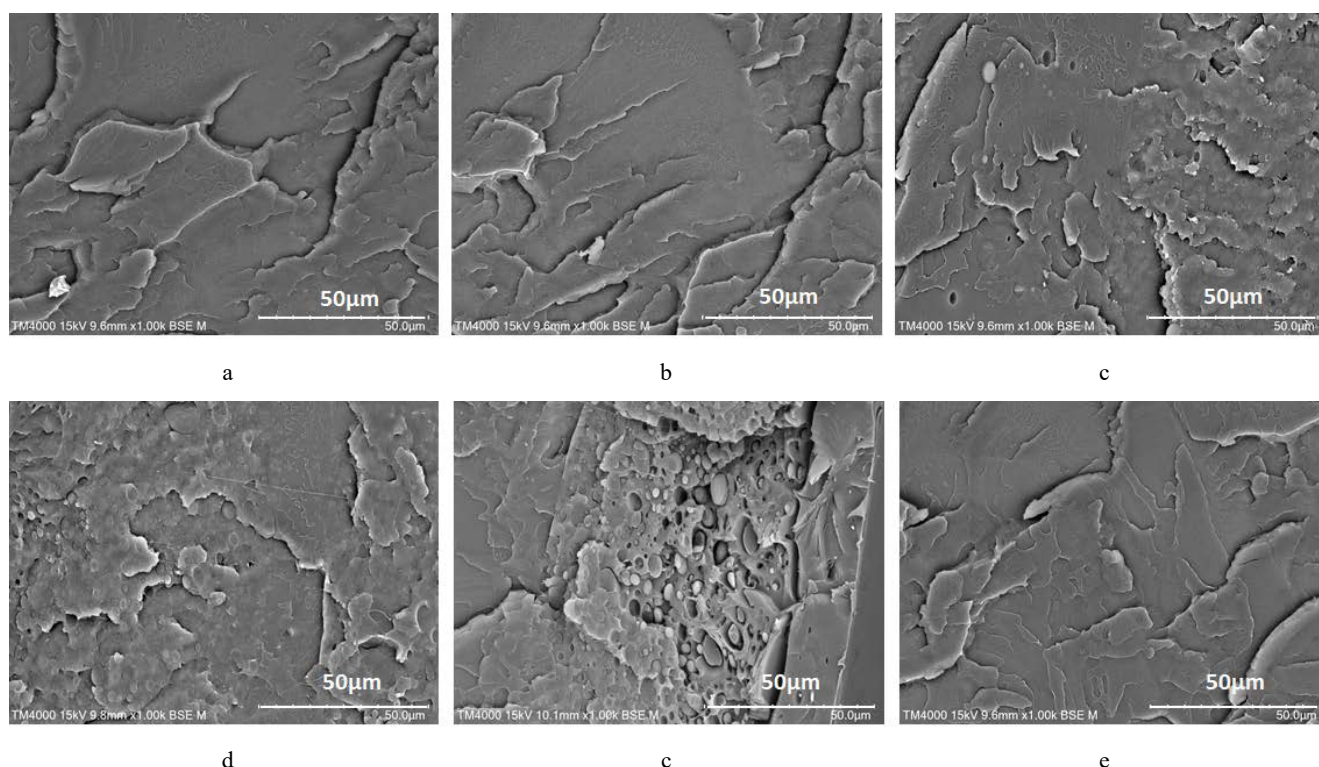

Fig. 6. Scanning electron micrographs of the quenched fractured surface: a – PLLA; b – ST; c – ST/10%PMMA; d – ST/30%PMMA; e – ST/50%PMMA; f – PMMA images at 1000× magnification
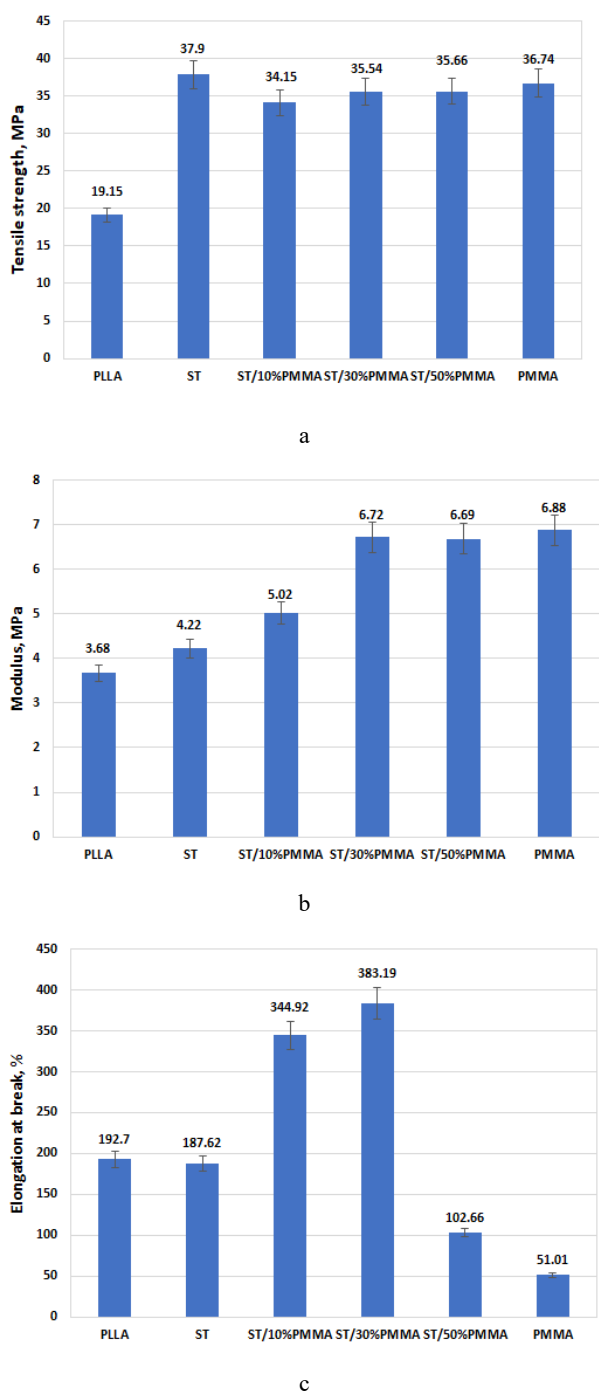
a

b

c

Fig. 7. Tensile properties of PLLA, ST, PMMA, and ST/PMMA blends: a – tensile strength; b – modulus of elasticity; c – elongation at break

3.6. Thermal Stability

The thermal stability was measured by thermal gravimetric analysis. Mass loss due to thermal decomposition was measured at temperatures from 30 to 600 °C [26]. Because the thermal stability of the 10, 30 and 50 % PMMA blends were not significantly different, only the ST/50% PMMA was compared with PLLA, ST and PMMA as shown in Fig. 8. The thermal decomposition temperatures (based on the 5 % loss criterion, T5%) of PLLA was 334 °C, the stereocomplex, ST, was 354 °C, and the PMMA was 362 °C. Purnama and Kim [27] also

reported that the stereocomplex decomposition temperature was higher than the PLLA homopolymer [27].
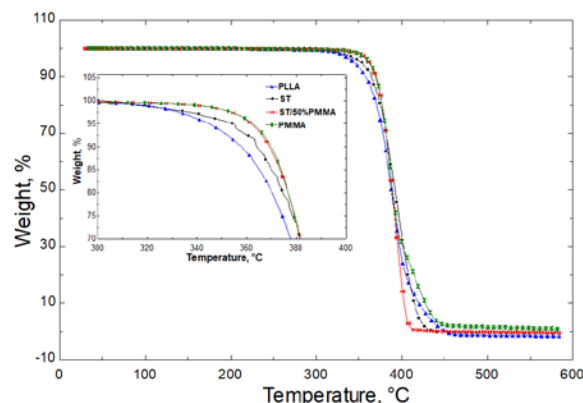

Fig. 8. TGA curves for PLLA, ST, PMMA and ST/50%PMMA blends

Moreover, when ST was mixed with 50% PMMA, T5% of the blend material was ~ 361 °C, higher than the stereocomplex (ST), but slightly less than PMMA. As the PMMA content increased, the dispersion of PMMA increased overall thermal stability, reflected in a higher decomposition temperature, possibly due to the higher thermal stability of PMMA itself. Teoh et al. [28] also reported that the addition of PMMA to pure PLLA improved thermal stability.

4. CONCLUSIONS

Films were formed from PLLA, PDLA and PMMA blends by dissolving them in chloroform at room temperature and cast. FTIR spectra showed intermolecular reactions between the stereocomplex and PMMA blends. XRD diffraction peaks of the stereocomplex/PMMA blends gradually became smaller as the PMMA content increased showing that the crystallinity of the polymer composites decreased and at high PMMA concentrations the films were essentially amorphous. DSC studies for the stereocomplex and PMMA added at 10 to 50 wt.% found that there were almost complete stereocomplex polylactide crystallites. The stereocomplex structure improved the melting temperature to be ~ 50 °C higher than pure PLLA. In SEM images, when the amount of PMMA was increased, phase separations were seen in the stereocomplex/PMMA blends. Tensile modulus and elongation-at-break of the blended materials improved, but tensile strength did not change significantly, demonstrating that the PMMA interfered with the stereocomplex chains, to enhance physical cross-linking points and markedly confine polymer chain motion. However, toughness diminished as the amount of PMMA was increased above 30 wt.%. The optimal addition was 30 wt.% leading to the best elongation at break and toughness. Additionally, the thermal stability of the polymer blends improved with the addition of PMMA and made them more suitable for several common applications, *e.g.* for packaging and protection of manufactured.

REFERENCES

1. **Zhang, G., Zhang, J., Wang, S., Shen, D.** Miscibility and Phase Structure of Binary Blends of Polylactide and Poly (Methyl Methacrylate) *Journal of Polymer Science Part B: Polymer Physics* 41 (1) 2003: pp. 23 – 30.
https://doi.org/10.1002/polb.10353

2. **Han, Y., Shi, J., Mao, L., Wang, Z., Zhang, L.** Improvement of Compatibility and Mechanical Performances of PLA/PBAT Composites with Epoxidized Soybean Oil as Compatibilizer *Industrial & Engineering Chemistry Research* 59 (50) 2020: pp. 21779 – 21790.
https://doi.org/10.1021/acs.iecr.0c04285

3. **Imre, B., Renner, K., Pukánszky, B.** Interactions, Structure and Properties in Poly (lactic acid)/thermoplastic Polymer Blends *Express Polymer Letters* 8 (1) 2014: pp. 2 – 14.
https://doi.org/10.3144/expresspolymlett.2014.2

4. **Bao, R.Y., Yang, W., Jiang, W.R., Liu, Z.Y., Xie, B.H., Yang, M.B., Fu, Q.** Stereocomplex Formation of High-Molecular-Weight Polylactide: A Low Temperature Approach *Polymer* 53 (24) 2012: pp. 5449 – 5454.
https://doi.org/10.1016/j.polymer.2012.09.043

5. **Ahmed, J., Varshney, S.K., Janvier, F.** Rheological and Thermal Properties of Stereocomplexed Polylactide Films *Journal of Thermal Analysis and Calorimetry* 115 (3) 2014: pp. 2053 – 2061.
https://doi.org/10.1007/s10973-013-3234-9

6. **De Arenaza, I.M., Sarasua, J.R., Amestoy, H., Lopez-Rodriguez, N., Zuza, E., Meaurio, E., Meyer, F., Santon, J.I., Jean-Marie, R., Dubois, P.** Polylactide Stereocomplex Crystallization Prompted by Multiwall Carbon Nanotubes *Journal of Applied Polymer Science* 130 (6) 2013: pp. 4327 – 4337.
https://doi.org/10.1002/app.39721

7. **Samuel, C.D., Cayuela, J., Barakat, I., Müller, A.J., Raquez, J.M., Dubois, P.** Stereocomplexation of Polylactide Enhanced by Poly (methyl methacrylate): Improved Processability and Thermomechanical Properties of Stereocomplexable Polylactide-based Materials *ACS Applied Materials & Interfaces* 5 (22) 2013: pp. 11797 – 11807.
https://doi.org/10.1021/am403443m

8. **Sarasua, J.R., Arraiza, A.L., Balerdi, P., Maiza, I.** Crystallinity and Mechanical Properties of Optically Pure Polylactides and Their Blends *Polymer Engineering & Science* 45 (5) 2005: pp. 745 – 753.
https://doi.org/10.1002/pen.20331

9. **Paydayesh, A., Azar, A.A., Arani, A.J.** Investigation the Effect of Graphene on The Morphology, Mechanical and Thermal Properties of PLA/PMMA Blends *Clinical and Experimental Nephrology* 37 2015: pp. 15 – 22.
https://doi.org/10.5902/2179460X20823

10. **Quynh, T.M., Mai, H.H., Lan, P.N.** Stereocomplexation of Low Molecular Weight Poly (L-lactic acid) and High Molecular Weight Poly (D-lactic acid), Radiation Crosslinking PLLA/PDLA Stereocomplexes and Their Characterization *Radiation Physics and Chemistry* 83 2013: pp. 105 – 110.
https://doi.org/10.1016/j.radphyschem.2012.10.002

11. **Srithep, Y., Pholharn, D.** Plasticizer Effect on Melt Blending of Polylactide Stereocomplex *E-Polymers* 17 (5) 2017: pp. 409 – 416.
https://doi.org/10.1515/epoly-2016-0331

12. **Pholharn, D., Srithep, Y., Morris, J.** Melt Compounding and Characterization of Poly (lactide) Stereocomplex/Natural Rubber Composites *Polymer Engineering & Science* 58 (5) 2018: pp. 713 – 718.
https://doi.org/10.1002/pen.24603

13. **Xiao, H., Lu, W., Yeh, J.T.** Effect of Plasticizer on The Crystallization Behavior of Poly (lactic acid) *Journal of Applied Polymer Science* 113 (1) 2009: pp. 112 – 121.
https://doi.org/10.1002/app.29955

14. **Tsuji, H.** Poly (lactide) Stereocomplexes: Formation, Structure, Properties, Degradation, and Applications *Macromolecular Bioscience* 5 (7) 2005: pp. 569 – 597.
https://doi.org/10.1002/mabi.200500062

15. **Diken, M.E., Doğan, S., Turhan, Y., Doğan, M.** Biological Properties of PMMA/nHAp and PMMA/3-APT-nHAp Nanocomposites *International Journal of Polymeric Materials and Polymeric Biomaterials* 67 (13) 2018: pp. 783 – 791.
https://doi.org/10.1080/00914037.2017.1378885

16. **Samuel, C., Raquez, J.M., Dubois, P.** PLLA/PMMA blends: A Shear-Induced Miscibility with Tunable Morphologies and Properties? *Polymers* 54 (15) 2013: pp. 3931 – 3939.
https://doi.org/10.1016/j.polymer.2013.05.021

17. **Ikada, Y., Jamshidi, K., Tsuji, H., Hyon, S. H.** Stereocomplex Formation between Enantiomeric Poly (lactides) *Macromolecules* 20 (4) 1987: pp. 904 – 906.
https://doi.org/10.1021/ma00170a034

18. **Srithep, Y., Pholharn, D., Turng, L.S., Veang-in, O.** Injection Molding and Characterization of Polylactide Stereocomplex *Polymer Degradation and Stability* 120 2015: pp. 290 – 299.
https://doi.org/10.1016/j.polymdegradstab.2015.07.017

19. **Srithep, Y., Pholharn, D., Turng, L.S.** Characterization of Stereocomplex Polylactide/Nanoclay Nanocomposites *International Polymer Processing* 32 (1) 2017: pp. 121 – 128.
https://doi.org/10.3139/217.3310

20. **Gonzalez-Garzon, M., Shahbikian, S., Huneault, M.A.** Properties and Phase Structure of Melt-Processed PLA/PMMA Blends *Journal of Polymer Research* 25 (2) 2018: pp. 1 – 13.
https://doi.org/10.1007/s10965-018-1438-1

21. **Liu, T., Xiang, F., Qi, X., Yang, W., Huang, R., Fu, Q.** Optically Transparent Poly (methyl methacrylate) with Largely Enhanced Mechanical and Shape Memory Properties via In-situ Formation of Polylactide Stereocomplex in the Matrix *Polymer* 126 2017: pp. 231 – 239.
https://doi.org/10.1016/j.polymer.2017.08.047

22. **Xu, H., Tang, S., Chen, J., Yin, P., Pu, W., Lu, Y.** Thermal and Phase-separation Behavior of Injection-molded Poly (L-lactic acid)/Poly (D-lactic acid) Blends with Moderate Optical Purity *Polymer Bulletin* 68 (4) 2012: pp. 1135 – 1151.
https://doi.org/10.1007/s00289-011-0673-y

23. **Tsuji, H., Fukui, I.** Enhanced Thermal Stability of Poly (lactide) s in the Melt by Enantiomeric Polymer Blending *Polymer* 44 (10) 2003: pp. 2891 – 2896.
https://doi.org/10.1016/S0032-3861(03)00175-7

24. **Mehrabi Mazidi, M., Edalat, A., Berahman, R., Hosseini, F.S.** Highly-Toughened Polylactide-(PLA-) Based Ternary Blends with Significantly Enhanced Glass Transition and Melt Strength: Tailoring the Interfacial Interactions, Phase Morphology, and Performance *Macromolecules* 51 (11) 2018: pp. 4298 – 4314.
https://doi.org/10.1021/acs.macromol.8b00557

25. **López-Rodríguez, N., Martínez de Arenaza, I., Meaurio, E., Sarasua, J.R.** Improvement of Toughness by

Stereocomplex Crystal Formation in Optically Pure Polylactides of High Molecular Weight *Journal of the Mechanical Behavior of Biomedical Materials* 37 2014: pp. 219 – 225.
https://doi.org/10.1016/j.jmbbm.2014.05.022

26. **Stephen, R., Jose, S., Joseph, K., Thomas, S., Oommen, Z.** Thermal Stability and Ageing Properties of Sulphur and Gamma Radiation Vulcanized Natural Rubber (NR) and Carboxylated Styrene Butadiene Rubber (XSBR) Lattices and Their Blends *Polymer Degradation and Stability* 91 (8) 2006: pp. 1717 – 1725.

https://doi.org/10.1016/j.polymdegradstab.2005.12.001

27. **Purnama, P., Kim, S.H.** Biodegradable Blends of Stereocomplex Polylactide and Lignin by Supercritical Carbon Dioxide-Solvent System *Macromolecular Research* 22 (1) 2014: pp. 74 – 78.
https://doi.org/10.1007/s13233-014-2004-2

28. **Teoh, E., Mariatti, M., Chow, W.** Thermal and Flame Resistant Properties of Poly (lactic acid)/Poly (methyl methacrylate) Blends Containing Halogen-Free Flame Retardant Procedia *Chemistry* 19 2016: pp. 795 – 802.
https://doi.org/10.1016/j.proche.2016.03.087